Contemporary Engineering Sciences, Vol. 10, 2017, no. 4, 193 - 202
HIKARI Ltd, www.m-hikari.com
https://doi.org/10.12988/ces.2017.611172

A Selective Active Filter for the 5G in the mm-Wave Band in pHEMT Technology

Imane Halkhams

LTTI, USMBA, Fez Morocco

Said Mazer, Moulhime El Bekkali, Wafae El Hamdani

LTTI, USMBA, Fez Morocco

Mahmoud Mehdi

Microwaves Laboratory, Faculty of Sciences, Lebanese University, Lebanon

Farid Temcamani

QUARTZ EA Laboratory ENSEA, France

Abstract

The modern telecommunication systems such as mobile radio network, wireless and satellites require the use of tunable high selective filters with a high quality factor Q. Unlike large sized passive filters whose frequency is difficult to tune, active inductor based filters have lots of benefits such as electronic frequency tuning, simplicity of integration and minimizing size. However, the intrinsic losses of the transistors limit the quality factor and the energy consumption remains significant. To remedy, various techniques exist in literature to boost Q including biasing conditions optimization in order to save energy and improve the quality factor of the filter. The centre frequency tuning requires varactors widely used in filtering and low noise amplifier circuits. In this way the frequency may be varied without affecting the quality factor of the filter. In this paper an active filter using 0.15 μm PHEMT technology is proposed with a centre frequency of 38 GHz for use in the next 5 generation of mobile network system. The aforementioned filter presents a high quality factor, a very good out-of-band rejection

and very low noise figure. This filter will be used in the implementation of high frequency transceivers in the millimetre band.

Keywords: Active filter; active inductor; 0.15 µm PHEMT; frequency tuning; quality factor

1 Introduction

The millimetre band is increasingly attracting the interest of wideband applications such as WPAN around 60 GHz [1], [2] and 5G between 5GHz and 40 GHz [3]. Implementation of lossless high selective filters is becoming more challenging due to millimetre band high atmospheric attenuation in particular signals in the range of 57-64 GHz that are subject to severe attenuation because of their absorption by oxygen molecules [4]. Active inductor based active filters are widely used for filtering applications in the S_band between 2 and 4 GHz, their frequency tuning ease makes them very suitable for multi-band applications. Their replacement of the classical passive filters allowed them to reach very high selective frequencies, but they still need enhancements to remedy to loss and noise limitations caused by active components in order to reach the millimetre band. In mobile systems, the growing demand for applications requiring constant connectivity and the demand for large bandwidths to cover the needs for high data rates require the migration to 5G that promises high capabilities such as high mobile communication rates of up to several gigabit data per second and low latency. As the frequency range allocated to 5G is not being defined yet (Fig. 1.), the entire spectrum of 1GHz to 100 GHz is currently considered [5].

Fig. 1. The expected spectrum for 5G wireless

Currently, a vast spectrum is available beyond 30 GHz and below 100 GHz, 5G wireless and cellular systems are most likely to operate at 28 GHz and 38 GHz [6]. Based on this assumption, this paper presents an active band-pass filter with a resonant frequency of 38 GHz. It uses an active inductor that provides the centre frequency. The latter is tuned due to a varactor that allows constant bandwidth over the tuning range. Biasing conditions and active matching networks were used and optimized to obtain the best performances, namely high centre frequency, low noise figure, out-of-band rejection and system stability.

2 Active inductor principle

High quality factor integrated band-pass filters based on resonator theory using both passive and active inductors have been widely used in multi standard

applications and are increasingly enhanced to reach high quality factor and selectivity. Passive inductors are bulky and cannot be easily tuned in frequency; their large size increases therefore losses and the cost of the circuit.
Unlike passive inductors, active inductors are increasingly used because of their small size, ease of tuning and integration while offering a high quality factor [7] [8]. The inductance is an essential element in the design of LNAs and oscillators used in the receiving chain. To implement an active inductance, several topologies are implemented. In our research, we study the active inductor based on gyrator as stated by Wu Yue [9]. The gyrator was invented by Bernard D. H. Tellegen (1900-1990). Its symbol is given in Fig. 2.

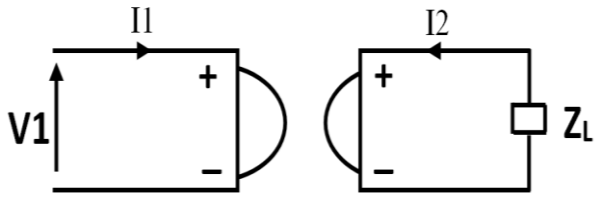

Fig. 2. Gyrator closed on impedance

It was first designed for low frequency applications where transconductance operational amplifiers were used to simulate grounded or floating active inductors using external built-in capacitances. These circuits were subsequently upgraded in order to reach high frequencies. The gyrator considered as a 2-port component, when closed on impedance, is described by the following impedance matrix:

$$\begin{bmatrix} V1 \\ V2 \end{bmatrix} = [Z] \begin{bmatrix} I1 \\ I2 \end{bmatrix} = \begin{bmatrix} Z11 & Z12 \\ Z21 & Z22 \end{bmatrix} \begin{bmatrix} I1 \\ I2 \end{bmatrix} \quad (1)$$

This equation stipulates that there is no energy generated, stored or dissipated, since the input power is equal to the output power. When the impedance is capacitive, the input impedance of the circuit is as follows:

$$Zin = \frac{Rg^2}{Zc} = Rg^2.Cp \quad (2)$$

where Rg is the gyration resistance [10]. This equation means that when the ideal gyrator is closed on a capacitance, it simulates the effect of the effect of an inductive impedance of value:

$$L = Rg^2.C \quad (3)$$

This equation illustrates the possibility of using ideal gyrators in combination with capacitors in order to simulate inductors, hence the term active inductor.
Active inductors based on transistors only and using internal capacitance have been a giant step towards system integration. They are widely used in the implementation of preselective filters, bandpass filters, LNAs and oscillators, replacing the Standard SAW filters. All these implementations exploit the inductive effect and the selectivity around the resonant frequency [11]. In the following, we use the principle of the gyrator to design an active band-pass filter

based on active inductance. Our objective is to choose an electronically tunable topology and to adapt it to high frequencies in order to meet the specifications of the fifth generation. Our choice is based on the topology presented by Wu Yue [9] (Fig.3).

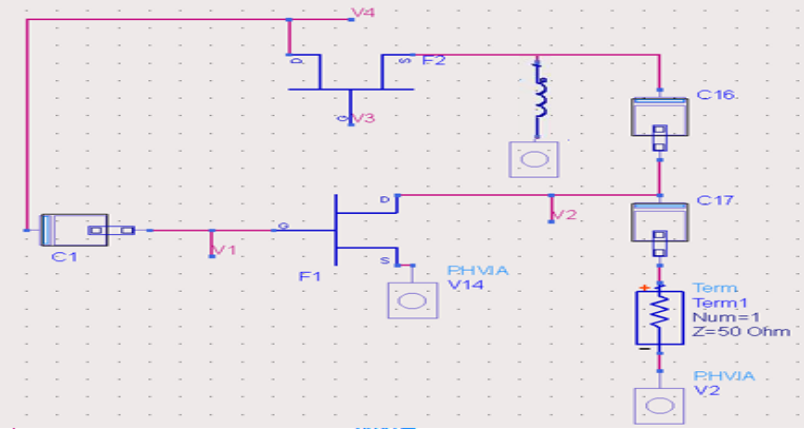

Fig. 3 Active inductor

We used in the simulations a nonlinear model of the Ga-As pHEMT 0.15 µm transistor delivered by the foundry United Monolithic Semiconductors (UMS) [12], whose characteristics are given in table I.

Table I: UMS 0.15 µm characteristics

Characteristic	Value
Cut-Off Frequency (FT)	110 GHz
Power Density	300 mW/mm
Idss	550 (mA/mm)
Vpinch	-0.7 V

The active inductance is constituted by a common source transistor M, in feedback with another transistor mounted as a common gate M. The two transistors constitute a gyrator which transforms the internal capacitance Cgs (between gate and source) of the first transistor into an inductor. The equivalent small signal circuit of the inductor is given in Fig. 4.

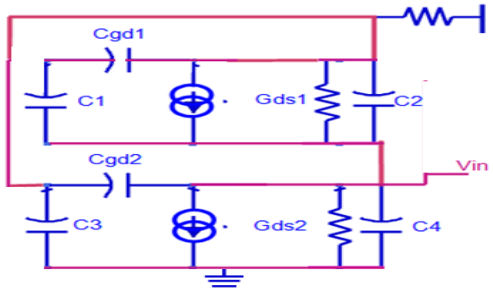

Fig. 4 Active inductor small signal equivalent circuit

The input admittance Yin calculated from Fig. 4 is given by (4):

$$\mathrm{Yin} = gm1 + j.w.Cgs1 + \frac{1}{\frac{gds1+R^{-1}}{gm1.gm2} + j.w.\frac{Cgs2}{gm1.gm2}} \quad (4)$$

In investigating equation (4), four terms can be deduced (5). The equation is a second order transfer function whose terms constitute a parallel RLC resonator.

$$L = \frac{Cgs2}{gm1.gm2};\ Rs = \frac{gds1+R^{-1}}{gm1.gm2};\ Rp = \frac{1}{gm1};\ Cp = Cgs1 \quad (5)$$

The RLC circuit may be considered as an equivalent inductor if the operating frequency is lower than the resonant frequency. The series and parallel resistors are the source of the losses of the RLC circuit. The approach adopted for measuring the elements of the equivalent circuit is based on the extraction method of the intrinsic parameters of the transistor cited hereinafter.

3 Extraction of the intrinsic parameters of the transistor

By studying the small signal circuit of the transistor (Fig. 5), the equations of the latter using the Y matrix are given by (6):

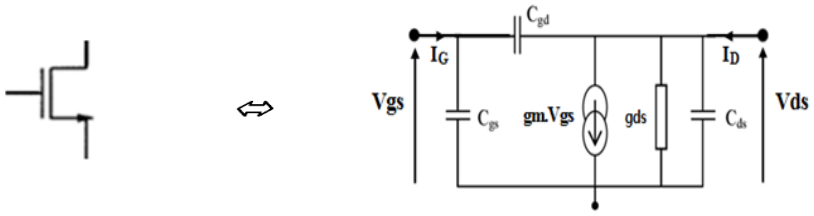

Fig. 4 Symbol of the transistor and small equivalent signal circuit

$$\begin{cases} IG = Y11.VGS + Y12.VDS \\ ID = Y21.VGS + Y22.VDS \end{cases} \quad (6)$$

When the voltage VDS = 0, Y11 and Y21 are expressed as:

$$Y11 = j.\omega.(Cgs + Cgd) \quad ; \quad Y21 = gm - j.\omega.Cgd \quad (7)$$

When the voltage VGS = 0, Y12 is expressed as:

$$Y12 = -j.\omega.Cgd \quad ; \quad Y22 = gds + j.\omega.(Cds + Cgd) \quad (8)$$

For a given frequency, the intrinsic parameters of the transistor are calculated and then used in the parameterization of the elements of the equivalent circuit. The simulations of the two circuits of the active inductor using pHEMT and the equivalent RLC circuit calculated from the intrinsic elements of the transistor are

given by Fig. 6. Several adjustments due to the inaccuracy of the curves caused by the neglected parasitic capacitances of the non-linear transistor have been made;

we obtain two perfectly concordant curves:

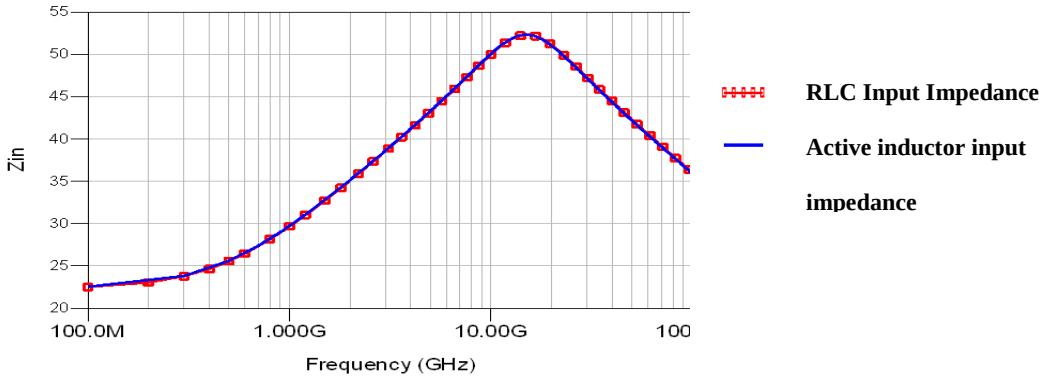

Fig. 6 Input impedance of RLC and AI circuit

The first simulations show a resonant frequency of 13 GHz, with an inductive effect above it and a capacitive effect beyond it.

4 Designed active filter

As we have demonstrated, active inductor constitutes the main element in a structure which performs the filtering operation by delivering the resonance frequency. In order to design an active bandpass filter using this active inductor structure, adaptation stages must be inserted in the input and output. In addition, the frequency tuning circuit will also be used in the design of the final filter with the same motivations. The input and output matching stages are located on either side of the designed filter (Fig. 7). The input component upstream of the active inductor makes it possible to deliver an impedance of 50Ω to the preceding stage, while the output buffer, downstream of the filter, makes it possible to approach the reference impedance 50Ω on the load side.

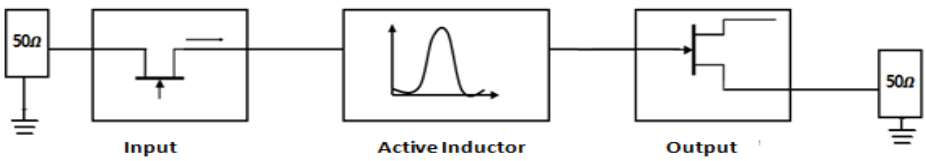

Fig. 7 Symbol of the transistor and small equivalent signal circuit

Input and output adaptation play a very important role in the response of the final filter as the addition of adaptation stages directly influences its performance [13] [14]. Then, the choice of input and output buffers must be thoroughly studied so that they fulfil their role of adaptation without changing other critical characteristics

such as the central frequency. Several topologies have been proposed in the literature, mainly in passive circuits [15], which allow a good linearity, but are inadequate for multi-standard applications, but also in active circuits which allow the stability of the circuit over a wide range of Frequencies [16]. The topology adopted for active input adaptation consists of a transistor mounted as a common gate. It has the advantage of having a low input impedance and a very high output impedance. For a low value of capacitance Cgs and a transconductance of the order of 20 mS, the input impedance becomes very close to 50Ω [17]. For the output, unlike the previous structure, the common drain circuit has an infinite input impedance on the side of the active inductor (resonator) and an output impedance of the order of 1/ gm on the load side. The optimization of the input and output buffers means choosing an optimum operating point in the saturation region in order to reduce the sensitivity of the frequency caused by a variation in the load. In this context, a simulation study was conducted to choose the optimal point. To this is added the effect of the coupling capacitor which isolates the continuous component and which must therefore be taken into account when tuning the filter frequency in order to have the desired central frequency.

5 Simulation results

The simulation of the S parameters of the topology cited is given in fig.8(a). This curve shows reciprocity on both sides of the central frequency of 38 GHz. This filter has low insertion losses <5 dB. The calculated bandwidth is 50 MHz in accordance with 5G standard [18]. Input and output reflections are -16 dB on a band between 37 GHz and 39 GHz, allowing out-of-band rejection, thus meeting the requirements of selective filters and the IEEE standard for local and metropolitan area networks [19].

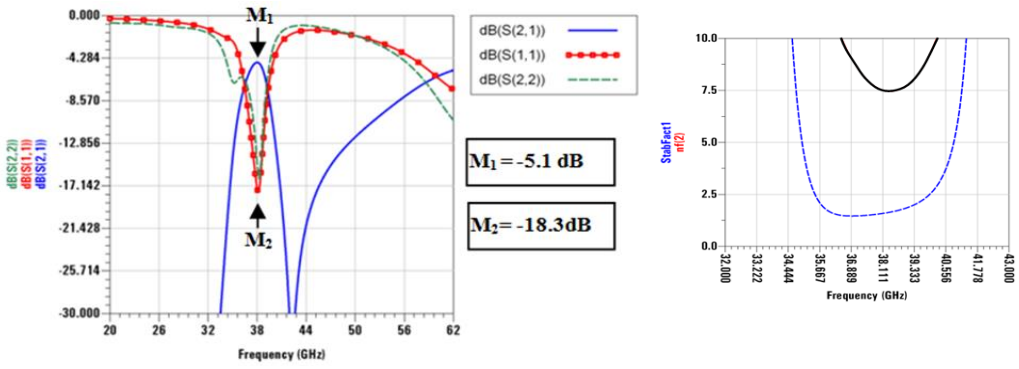

(a) **(b)**

Fig. 8 (a) The simulated filter S_Parameters (b) stability and noise simulations

The noise figure and the stability factor presented in Fig.8(b) describe the behaviour of the filter on the millimetre band. The stability of the filter is proven all around the resonant frequency with a minimum of 1.3 (> 1). The noise figure

has its minimum at the resonant frequency; however, it remains higher than the assumed value for similar active inductors. To characterize the microwave circuit performance, the effect of technological dispersion must be evaluated. The Monte Carlo analysis enables to randomly vary the values of circuit components specified by the UMS foundry, according to the statistical distributions to obtain the variation of the overall performance. We achieved a Monte Carlo analysis of 50 iterations shown on Fig. 9 (a).

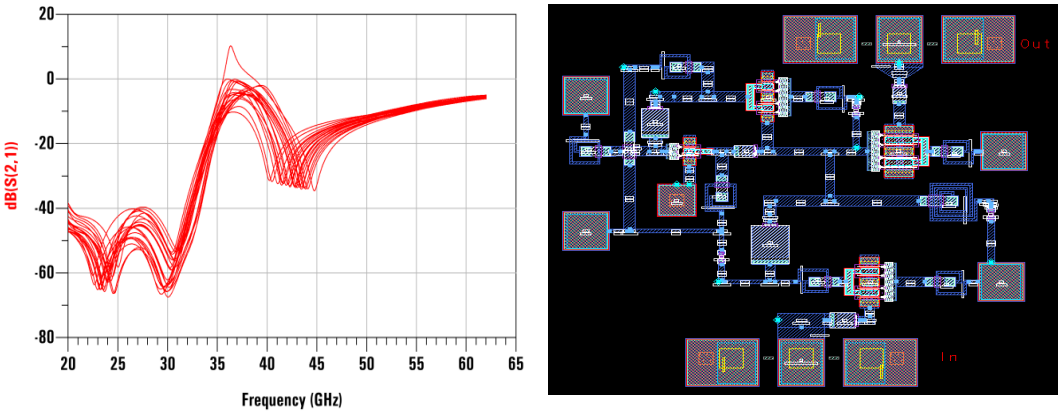

(a) **(b)**

Fig.9 (a) Monte Carlo analysis results (b) filter layout

We observe that the results of the iterations have almost the same amplitude with a variation of the centre frequency between 36 GHz and 40 GHz. This variation can be corrected easily by changing the voltage of the varactor to change the operating frequency. The layout of the designed filter is shown on Fig. 9 (b) with the dimensions 987 × 952 µm2.

6 Conclusion and Prospects

As an overview of this article, active inductor based active filters replacing passive filters are of great interest in terms of quality factor, large frequency tuning range, ability to achieve high values of inductance and ease of integration. Reaching high frequencies in the millimetre band is a challenging issue. Due to the proposed topology a centre frequency of 38 GHz is obtained with high out-band rejection. The technology pHEMT from UMS foundry was used in this study pHEMT based filter appears to fulfil 5G requirements, but displays high noise figure, which calls for further noise study.

References

[1] Y. Lin, C. Yo Lee, 9.99 mW 4.8 dB NF 57–81 GHz CMOS low-noise amplifier for 60 GHz WPAN system and 77 GHz automobile radar system,

Microwave and Optical Technology Letters, **57** (2015), no. 3, 594–600. https://doi.org/10.1002/mop.28898

[2] C. N. Deshmukh, V. T. Ingole, DWT-OFDM Diversity for TSV-Model Based 60 GHz WPAN System, *International Journal of Advanced Research in Computer and Communication Engineering*, **4** (2015), no. 1, 101-110. https://doi.org/10.17148/ijarcce.2015.4121

[3] G. Bochechka, V. Tikhvinskiy, Spectrum occupation and perspectives millimeter band utilization for 5G networks, Proceedings of the 2014 ITU Kaleidoscope Academic Conference, IEEE, St. Petersburg, 2014, 69-72. https://doi.org/10.1109/kaleidoscope.2014.6858482

[4] Kao-Cheng Huang, Zhaocheng Wang, *Millimeter Wave Communication Systems*, Wiley-IEEE Press, 2011. https://doi.org/10.1002/9780470889886

[5] Ericsson Inc, 5G radio access, White Paper Uen 284 23-3204 Rev B, Ericsson Inc,Stockholm, Stockholm, Sweden, 2015.

[6] Ahmed Iyanda Sulyman, AlMuthanna T. Nassar, Mathew K. Samimi et al., Radio Propagation Path Loss Models for 5G Cellular Networks in the 28 GHz and 38 GHz Millimeter-Wave Bands, *IEEE Communications Magazine*, **52** (2014), no. 9, 78 – 86. https://doi.org/10.1109/mcom.2014.6894456

[7] R.K. Lamba, C.H. Vithalani, Active Inductor Designs for RF CMOS Receiver Front-End, *International Journal of Applied Engineering Research*, **11** (2016), no. 2, 904-908.

[8] M. Pandey, A. Canelas, R. Póvoa, J. A. Torres, J.C. Freire, N. Lourenço and N. Horta, Design and Application of a CMOS Active Inductor at Ku Band based on a multi-objective optimizer, *Integration, the VLSI Journal*, **55** (2016), 330-340. https://doi.org/10.1016/j.vlsi.2016.06.007

[9] Y. Wu, M. Ismail et al., RF Bandpass Filter Design Based on CMOS Active Inductors, *IEEE Transactions on Circuits and Systems II: Analog and Digital Signal Processing*, **50** (2003), no. 12, 942–949. https://doi.org/10.1109/tcsii.2003.820235

[10] Paul Bildstein, Synthèse et réalisation des filtres actifs, Techniques de l'Ingénieur, traité Électronique.

[11] Cristian Andriesei, Liviu Goras, On Frequency and Quality Factor Independent Tuning Possibilities for RF Band-pass Filters with Simulated

Inductors, *Romanian Journal of Infrmation Science and Technology*, **11** (2008), no. 4, 367-382.

[12] United Monolithic Semiconductors, UMS foundry services, GaAs & GaN, 2013-2014.

[13] Mohammed Lahsaini, Lahbib Zenkouar, Interdigital Filters for Broadband Impedance Matching of Microwave Amplifiers, *International Journal on Communications Antenna and Propagation*, **5** (2015), no. 1, 21-27. https://doi.org/10.15866/irecap.v5i1.4905

[14] A. Saberkari, S. Ziabakhsh, H. Martinez, E. Alarcón, Active inductor-based tunable impedance matching network for RF power amplifier application, *Integration, the VLSI Journal*, **52** (2016), 301–308. https://doi.org/10.1016/j.vlsi.2015.07.013

[15] Ji-Kang Nai, Y. Hsiao, Y. Wang, Y. Lin, H. Wang, A 2.8-6 GHz High-Efficiency CMOS Power Amplifier with High-order Harmonic Matching Network, *IEEE MTT-S Microwave Symposium (IMS)*, IEEE, 2016. https://doi.org/10.1109/mwsym.2016.7540306

[16] M. Arif, S. Bhuiyan, J. Chew, M. Ibne Reaz, N. Kamal, Design of an active inductor based LNA in Silterra 130 nm CMOS process technology, *Journal of Microelectronics, Electronic Components and Materials*, **45** (2015), no. 3, 188–194.

[17] I.D. Robertson, S. Lucyszyn, *RFIC and MMIC Design and Technology*, IEE Circuits, Devices and Systems Series, IET, 2001. https://doi.org/10.1049/pbcs013e

[18] T. S. Rappaport et al., Millimeter wave mobile communications for 5G cellular: It will work!, *IEEE Access*, **1** (2013), 335-349. https://doi.org/10.1109/access.2013.2260813

[19] Ofcom, Laying the foundations for next generation mobile services: Update on bands above 6 GHz, IEEE Standard For Information Technology Local and Metropolitan Area Networks Specific Requirements –2015. 1-320, 7.

Received: November 19, 2016; Published: January 19, 2017